Approximate analytical solution for nuclear matter in a mean-field Walecka model and Coester line behavior

A. Delfino, J. B. Silva, and M. Malheiro
Instituto de Física, Universidade Federal Fluminense, Av. Litorânea s/n, 24210-150 Boa Viagem, Niterói RJ, Brazil
(Received 14 November 2005; published 29 March 2006)

We study nuclear matter, at the mean-field approximation, by considering as equal the values of the scalar and the vector density in the Walecka model, which is a very reasonable approximation up to the nuclear matter saturation density. It turns out that the model has an analytical solution for the scalar and vector couplings as functions only of the nuclear matter density and binding energy. The nuclear matter properties are very close to the original version of the model. This solution allows us to show that the correlation between the binding energy and the saturation density is Coester line like. The liquid-gas phase transition is also studied and the critical and flash temperatures are again very similar to the original ones.

DOI: 10.1103/PhysRevC.73.037311 PACS number(s): 21.65.+f, 21.30.Fe, 21.45.+v

At the mean-field level the linear σ-ω (or Walecka) model [1] explains satisfactorily many properties of nuclear matter and finite nuclei. This model employs nucleons and mesons as degrees of freedom, is renormalizable, and has two free parameters to fit. The sources for the fields are the scalar (ρ_s) and the vector (ρ) densities associated with the Lorentz scalar (S) and vector (V) interactions. An interesting result of this model was to show the relativistic mechanism for nuclear matter saturation. It occurs at a saturation density ρ_0, for which the S and V potentials largely cancel each other out.

For infinite nuclear matter in the Walecka model, the mean-field vector and scalar potentials are $V = C_v^2\rho/M^2$ and $S = -C_s^2\rho_s/M^2$ [1], where C_s and C_v are coupling constants that need to be found numerically in a self-consistent way to fit the correct nuclear matter binding energy and saturation density. Taking into account that, at ordinary nuclear densities, the scalar (ρ_s) and baryon (ρ) densities are equal to within a few percentages, we can assume that these potentials closely follow linearly the baryon density: $S = S_0\rho/\rho_0$ and $V = V_0\rho/\rho_0$, where S_0 and V_0 are the values of the potentials at the nuclear matter equilibrium density ρ_0.

The main purpose of this Brief Report is to show, using a reasonable approximation, that it is possible to find analytical expressions for the couplings constants C_s and C_v of the Walecka model that depend only on the nuclear matter binding energy and density. This analytical—and not numerical—solution allows us also to find a simple equation for nuclear matter binding energy as a function of the equilibrium density and the potential difference $V_0 - S_0$. This relation explains why the correlation between these two nuclear matter properties is Coester line like in the Walecka model, a behavior recently found only numerically for this model when $V_0 - S_0$ is kept fixed [2].

In this model, the one-body Dirac equation for the nucleons under scalar and vector mean-field potentials reads,

$$[\alpha \cdot \mathbf{p} + \beta(M + S) + V]\,\psi = E\psi, \tag{1}$$

where α and β are matrices. If we write ψ, a relativistic four component spinor, in terms of its small (χ) and large (ϕ) components, we get

$$\sigma \cdot \mathbf{p}\chi + (M + S + V)\phi = E\phi, \tag{2}$$

$$\boldsymbol{\sigma} \cdot \mathbf{p}\phi - (M + S - V)\chi = E\chi, \tag{3}$$

where $\boldsymbol{\sigma}$ is a three-vector whose components are the Pauli matrices.

Substituting χ from Eq. (3) into Eq.(2), one obtains

$$[(E - V)^2 - (M + S)^2 - \mathbf{p}^2]\phi = 0, \tag{4}$$

which gives us the known dispersion relation for the energy in the Walecka model. Let us define the quantities

$$\Sigma = V + S \qquad \text{and} \qquad \Delta = V - S, \tag{5}$$

which allow us to write, from Eqs. (2) and (3), a decoupled equation for the large component ϕ

$$\left[\frac{\mathbf{p}^2}{2M\left(1 - \frac{\epsilon' + \Delta}{2M}\right)} + \Sigma\right]\phi = \epsilon'\phi, \tag{6}$$

where $\epsilon' = M - E$ is the system binding energy.

The Eq. (4) describes a relativistic nucleon with an effective mass $M^* = M + S$ and energy $E^* = E - V$, whereas Eq. (6) suggests that the nucleon is described by the Hamiltonian

$$H = \Sigma + \frac{\mathbf{p}^2}{2\bar{M}} \tag{7}$$

that has a nonrelativistic form, where

$$\bar{M} = 2M\left(1 - \frac{\epsilon' + \Delta}{2M}\right), \tag{8}$$

may be understood as the nucleon effective mass. It is important to stress that Eqs. (4) and Eq. (6) are equivalents, despite the different M^* and $\bar{M}$ definitions. They are related by

$$\bar{M} = \tfrac{1}{2}[M^* + (M - V - \epsilon')]. \tag{9}$$

Now, we assume that the scalar and vector potentials closely follow the baryon density,

$$\Sigma = \Sigma_0\frac{\rho}{\rho_0} \qquad \text{and} \qquad \Delta = \Delta_0\frac{\rho}{\rho_0}, \tag{10}$$

where $\Delta_0 = V_0 - S_0$ and $\Sigma_0 = V_0 + S_0$ are free parameters. In this approximation $\rho_s = \rho$, we are neglecting higher-order terms in k_f/M, where k_f is the fermi momentum. However, this cannot be seen as a nonrelativistic approximation because the kinetic energy in Eq. (7) depends on the effective mass $\bar{M}$ and not on the bare nucleon mass M. Therefore, the kinetic term still has relativistic content.

Neglecting $\epsilon'/2M$ corrections, which are small, we obtain from Eq. (6) a nonrelativistic energy density

$$\mathcal{E} = \Sigma\rho + \frac{\gamma}{(2\pi)^3}\int \frac{k^2}{2\bar{M}} d^3k, \tag{11}$$

where γ is the degeneracy factor ($\gamma = 4$ for nuclear matter and $\gamma = 2$ for neutron matter) with a nucleon *effective* mass

$$\bar{M} = M\left(1 - \frac{\Delta}{2M}\right). \tag{12}$$

By minimization of $\mathcal{E}/\rho$ at $\rho = \rho_0$, and defining the binding energy $\mathcal{E}/\rho_0 - M = -B_0$, we obtain analytical expressions for Δ_0 and Σ_0:

$$\Delta_0 = 2M\left[1 + \frac{2E_f^o}{3B_0}\left(1 - \sqrt{1 + \frac{9B_0}{4E_f^o}}\right)\right], \tag{13}$$

and

$$\Sigma_0 = -B_0 - \frac{E_f^o}{1 - \Delta_0/2M}, \tag{14}$$

where

$$E_f^o = \frac{3}{10}\frac{k_f^{o2}}{M} \quad \text{and} \quad \rho_0 = \frac{\gamma}{6\pi^2}k_f^{o3} \tag{15}$$

are the Fermi kinetic energy and the equilibrium density respectively. Notice that by fixing B_0 and ρ_0, the parameters Δ_0 and Σ_0 are automatically determined.

The expressions for energy density and pressure are

$$\mathcal{E} = \Sigma_0\frac{\rho^2}{\rho_0} + \frac{3}{10M}\left(\frac{6\pi^2}{\gamma}\right)^{2/3}\left[\frac{\rho^{5/3}}{1 - \frac{\Delta_0\rho}{2M\rho_0}}\right], \tag{16}$$

and

$$P = \Sigma_0\frac{\rho^2}{\rho_0} + \frac{1}{5M}\left(\frac{6\pi^2}{\gamma}\right)^{2/3}\left[\frac{1 + \frac{\Delta_0\rho}{4M\rho_0}}{\left(1 - \frac{\Delta_0\rho}{2M\rho_0}\right)^2}\right]\rho^{5/3}. \tag{17}$$

We verify the thermodynamic consistency of the model through the calculation of the chemical potential,

$$\mu = \frac{\partial\mathcal{E}}{\partial\rho} = 2\Sigma_0\frac{\rho}{\rho_0} + \frac{1}{2M}\left(\frac{6\pi^2}{\gamma}\right)^{2/3}\left[\frac{1 - \frac{2}{5}\frac{\Delta_0\rho}{2M\rho_0}}{\left(1 - \frac{\Delta_0\rho}{2M\rho_0}\right)^2}\right]\rho^{2/3}, \tag{18}$$

that can also be obtained by $\mu = (\mathcal{E} + P)/\rho$.

We can solve Eqs. (13) and (14) to give Σ_0 and B_0 in terms of E_f^o and Δ_0,

$$\Sigma_0 = -E_f^o\frac{\frac{1}{3}\left(2 + \frac{\Delta_0}{2M}\right)}{\left(1 - \frac{\Delta_0}{2M}\right)^2}. \tag{19}$$

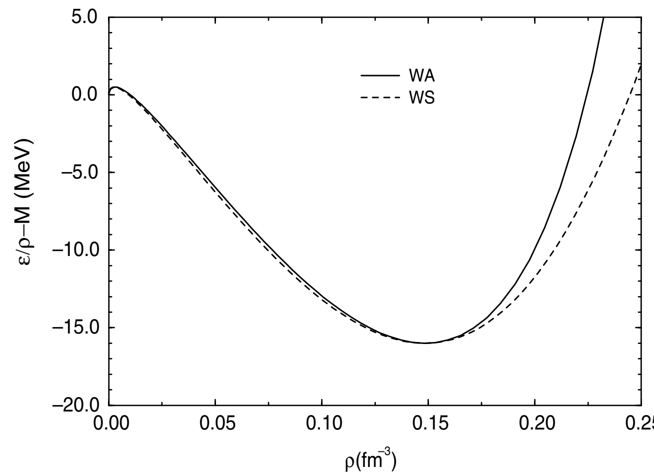

FIG. 1. Binding energy as a function of the density for the models WS and WA.

and

$$B_0 = \frac{E_f^o}{3}\frac{\left(\frac{2\Delta_0}{M} - 1\right)}{\left(1 - \frac{\Delta_0}{2M}\right)^2}. \tag{20}$$

We can also find an analytical expression for the incompressibility,

$$K = 9\left.\frac{\partial P}{\partial\rho}\right|_{\rho=\rho_0} = \frac{2E_f^o}{\left(1 - \frac{\Delta_0}{2M}\right)^3}\left[\frac{4\Delta_0}{M} + \frac{\Delta_0^2}{2M^2} - 1\right]. \tag{21}$$

It is important to notice that once ρ_0 is fixed, K depends only on Δ_0.

In Fig. 1, we present the binding energy curves for the original Walecka model (WS) and the approximate one (WA).

Notice how the approximate model presents a harder equation of state (EOS) than the Walecka original one. The proximity of the models suggests that the saturation mechanism of the Walecka model is the result of the increase of the kinetic energy coming from the relativistic corrections. This relativistic effect is still present after the approximation because, from Eq. (16), we see that the kinetic energy depends on the effective mass. The nonrelativistic limit, which is the same of the ordinary Walecka model, is to take $\Delta_0 = 0$. In this case $\bar{M} = M$ and Eq. (16) reduces to

$$\frac{\mathcal{E}}{\rho} = \Sigma_0\frac{\rho}{\rho_0} + \frac{3}{10M}\left(\frac{6\pi^2\rho}{\gamma}\right)^{2/3}. \tag{22}$$

The dominant term comes from the attractive part, collapsing the system for high values of ρ. This only shows the essential relativistic character of the Walecka model. The ordinary explanation for the saturation mechanism in the original WS model is that it occurs from the balance between the scalar and baryonic density in which the later one dominates at high density. However, because the results of WS and the approximate WA model are very similar, we are forced to conclude that, in fact, this mechanism occurs as a result of the increase of the kinetic energy that is sufficient to saturate the system. Looking at Eqs. (7) and (16) of the WA model, we identify Σ and Δ as the physical scales of the problem.

TABLE I. Equilibrium properties of nuclear matter obtained from WS and WA. Binding energy, incompressibility, and nucleon effective mass are given in MeV and ρ_0 is given in fm^{-3}.

Models	B_0	ρ_0	Σ_0	Δ_0	K	m^*
W	16.0	0.148	−77	785	551	0.539
WA	16.0	0.148	−53	813.7	656.6	0.566

We identify Σ as the nonrelativistic scale associated with the depth of the nuclear potential, whereas Δ, which saturates the model by the increase of kinetic energy, is the proper relativistic scale. This is the main reason why we wrote the model with those two potentials, instead of the usual scalar S and vector V potentials.

We present in Table I some bulk properties for the models and we can see how the results are close to each other.

To understand better the role played by the relativistic scale Δ_0 (the value of the potential Δ at the equilibrium density ρ_0), we see that in WA model it determines completely the incompressibility and also the nucleon effective mass once ρ_0 is fixed. It is also known that Δ_0 relates directly to the spin-orbit splitting in finite nuclei. The correlation between this splitting and the nucleon effective mass in equilibrium nuclear matter shows that the larger is the effective mass and the smaller is such splitting [3]. The WA model also shows this, because $\bar{M}$ decreases as Δ_0 increases. It is interesting to notice that if $\epsilon' = -B_0$ in Eq. (9), $\bar{M} = \frac{1}{2}(M^* + M_L^*)$, where $M_L^* = \sqrt{k_f^2 + (M+S)^2}$ is the Landau nucleon effective mass. We have also to point out that $\bar{M}$, which decreases linearly with the density, may hit negative values and it happens when $\rho/\rho_0 < (2M - B_0)/\Delta_0$. This restrict the validity of the *EOS* to $\rho/\rho_0 < 2.28$.

In Fig. 2, we present B_0 as a function of ρ_0 for different values of Δ_0. The curves show a correlation between B_0 and ρ_0, expressed in Eq. (20). It is known that an N-body calculation, using a two-nucleon potential model that fits two nucleon properties, furnishes a function $B_0(\rho_0)$. This intriguing result was analyzed by Coester *et al.* [4] in a two-nucleon model interaction by varying its tensor force contribution while keeping the deuteron binding energy fixed. They showed that $B_0(\rho_0)$ roughly follows a line. They have also observed the similarity of such a line with that constructed from B_0 and ρ_0 obtained from different calculations, using distinct two-nucleon potentials and far from the experimental point. Even modern calculations using BHF and including single-particle contribution in the continuum, change the results but keeps the correlation intact. These findings are shown in Fig. 2, in which the continue line originated from the WA model crosses the experimental point, by construction. Notice, however, how the curves from the WA model follow the slope of the points calculated with two-nucleon models. That is why we claim to have obtained a kind of Coester line correlation. It is interesting to point out that the relativistic effects of the WA models are also shown in Fig. 2, where the Coester line is shifted to the empirical region of saturation, provided the relativistic scale Δ is large. This suggests a Dirac structure for the nuclear potential with *large* scalar and vector parts [2].

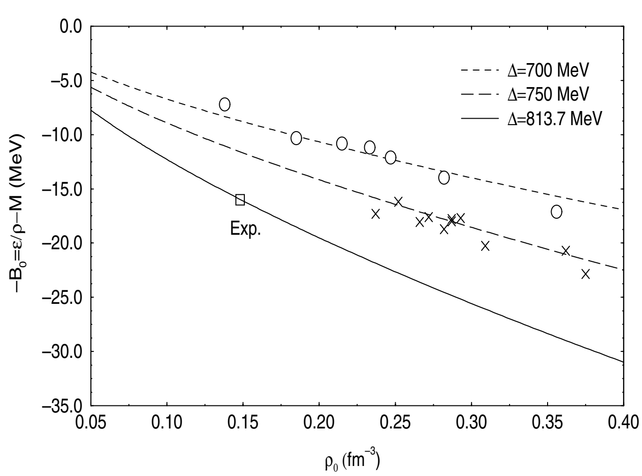

FIG. 2. Nuclear matter binding energy as a function of the saturation density for different values of Δ in WA model. Circles indicate calculations using RSC, Paris, HJ, AV14, Bonn A, B, and C, extracted from Ref. [5]. Nuclear matter calculations, including the single-particle continuum contribution, are shown with the × symbol.

TABLE II. Critical and flash parameters for WA and WS models. Temperature is given in MeV, density in fm^{-3}, and pressure in MeV/fm^3.

Parameter	Model	T	ρ	P
Critical	WS	18.35	0.064	0.414
	WA	16.6	0.066	0.441
Flash	WS	14.23	0.089	0
	WA	11.3	0.092	0

It is important to comment that our approximation should work even better in the case of nonlinear scalar coupling models [6], because they need less relativistic content to achieve saturation.

Just for the sake of completeness, we have also investigated WA model at finite temperature. We have introduced an ideal

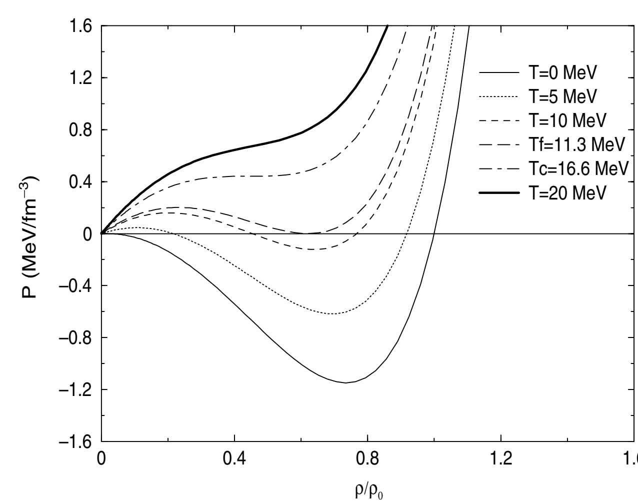

FIG. 3. Pressure as a function of ρ/ρ_0 for some isotherms. The temperature is in mega electron volts.

gas contribution ρkT in the *EOS* to calculate the critical parameters. We have also calculated the "flash" parameters. The "flash" temperature T_f is defined as the highest temperature at which a self-bound system can exist in hydrostatic equilibrium. The results are presented in Table II.

Again, we see how the critical and flash parameters obtained from the WA model are close to those of the *WS* model [7,8]. In Fig. 3, we display the pressure as a function of ρ/ρ_0 for some isotherms. The behavior is similar to a Van der Waals liquid-gas equation of state [7].

In summary, we showed that, when the scalar and the vector potentials follow the baryonic density, the Walecka model has an analytical solution for the scalar and vector couplings as functions only of the nuclear matter density and binding energy. The nuclear matter properties are very close to the original version of the model. This solution can also explain why the correlation between the binding energy and the saturation density is Coester line like. The critical and flash temperatures of the warm nuclear matter are also very similar to the original ones.

[1] B. D. Serot and J. D. Walecka, Adv. Nucl. Phys. **16**, 1 (1986).
[2] A. Delfino, M. Malheiro, V. S. Timoteo, and J. S. Sá Martins, Braz. J. Phys. **35**, 190 (2005).
[3] R. J. Furnsthal, J. J. Rusnak, and B. D. Serot, Nucl. Phys. **A632**, 607 (1997).
[4] F. Coester, S. Cohen, B. D. Day, and C. M. Vincent, Phys. Rev. C **1**, 769 (1970).
[5] R. Machleidt, Adv. Nucl. Phys. **19**, 189 (1989).
[6] J. Zimanyi and S. A. Moszkowski, Phys. Rev. C **42**, 1416 (1990).
[7] A. Delfino, C. T. Coelho, and M. Malheiro, Phys. Rev. C **51**, 2188 (1998).
[8] M. Malheiro, A. Delfino, and C. T. Coelho, Phys. Rev. C **58**, 426 (1998).